Field-induced interplanar magnetic correlations in the high-temperature superconductor $La_{1.88}Sr_{0.12}CuO_4$

A. T. Rømer,[1] P. J. Ray,[1] H. Jacobsen,[1] L. Udby,[1] B. M. Andersen,[1] M. Bertelsen,[1] S. L. Holm,[1] N. B. Christensen,[2] R. Toft-Petersen,[3] M. Skoulatos,[4] M. Laver,[2,4,*] A. Schneidewind,[5] P. Link,[6] M. Oda,[7] M. Ido,[7] N. Momono,[8] and K. Lefmann[1]

[1]*Nanoscience Center, Niels Bohr Institute, University of Copenhagen, DK-2100 Copenhagen, Denmark*
[2]*Department of Physics, Technical University of Denmark, DK-2800 Kongens Lyngby, Denmark*
[3]*Helmholtz Zentrum Berlin für Materialien und Energie, D-14109 Berlin, Germany*
[4]*Laboratory of Neutron Scattering, Paul Scherrer Institute, 5232 Villigen, Switzerland*
[5]*Jülich Centre for Neutron science (JCNS) at MLZ, Forschungszentrum Jülich GmbH, Outstation MLZ, Lichtenbergstrasse 1, 85747 Garching, Germany*
[6]*Heinz Maier-Leibnitz-Zentrum (MLZ), Technische Universität München, Lichtenberstrasse 1, 85747 Garching, Germany*
[7]*Department of Physics, Hokkaido University, Sapporo 060-0810, Japan*
[8]*Department of Applied Sciences, Muroran Institute of Technology, Muroran 050-8585, Japan*

(Received 23 December 2014; revised manuscript received 16 March 2015; published 11 May 2015)

We present neutron-scattering studies of the interplanar magnetic correlations in the high-temperature superconductor $La_{1.88}Sr_{0.12}CuO_4$ ($T_c = 27$ K). The correlations are studied both in a magnetic field applied perpendicular to the CuO_2 planes, and in zero field under different cooling conditions. We find that the effect of the magnetic field is to increase the magnetic scattering signal at all values of the out-of-plane wave vector L, indicating an overall increase of the magnetic moments. In addition, weak correlations between the copper oxide planes develop in the presence of a magnetic field. This effect is not taken into account in previous reports on the field effect of magnetic scattering, since usually only $L \approx 0$ is probed. Interestingly, the results of quench-cooling the sample are similar to those obtained by applying a magnetic field. Finally, a small variation of the incommensurate peak position as a function of L provides evidence that the incommensurate signal is twinned with the magnetic scattering from the dominant and subdominant structural twin displaying peaks at even and odd values of L, respectively, in our crystal.

DOI: 10.1103/PhysRevB.91.174507 PACS number(s): 74.25.Uv, 74.81.−g, 75.30.−m, 75.25.−j

I. INTRODUCTION

The interplay between magnetic ordering and superconductivity remains a topic of intense investigation in both cuprates and iron-based superconductors [1]. In the single-layer cuprate superconductor $La_{2-x}Sr_xCuO_4$ (LSCO), quasi-two-dimensional incommensurate (IC) magnetic order and fluctuations have been observed at a quartet of IC positions around the magnetic ordering vector in the parent compound La_2CuO_4 (LCO); i.e., $\mathbf{Q}_{IC} = (1 \pm \delta_H, \pm \delta_K, L)$ in orthorhombic notation [2–6]. In the doping range $0.06 \leqslant x \leqslant 0.13$ it was shown by Yamada *et al.* [7] that the incommensurability δ scales linearly with the doping, $\delta \approx x$. For doping levels close to $x = 0.125$, the superconducting critical transition temperature is somewhat suppressed [8], which is known as the 1/8 anomaly and presumably caused by stripe ordering [9–15]. The static magnetism in LSCO near $x = 0.125$, as well as its momentum space characteristics, has been previously studied in great detail [4,8,16].

Several experiments have shown that application of a magnetic field perpendicular to the CuO_2 planes leads to an enhancement of the elastic response from the magnetic IC order at $\mathbf{Q}_{IC}$ for doping values in a range around the 1/8 anomaly: $0.10 \leqslant x \leqslant 0.135$ [17–19]. In LSCO of higher doping no static order is present, but it has been shown that magnetic order can be induced by application of a magnetic field [20,21].

Previously, some of us studied the interplanar magnetic correlations in a crystal with doping value of $x = 0.11$ [22,23]. We observed that only the magnetic field component perpendicular to the CuO_2 plane, commonly referred to as the (a,b) plane, gives rise to an enhanced IC scattering, whereas the field component in the plane does not affect the magnetic IC signal. Further, the field-induced intensity was modulated along the c axis, indicating that interplanar spin correlations develop in the presence of a magnetic field perpendicular to the CuO_2 planes.

The observation of enhanced c-axis correlations raises a concern: Parts of, or in principle all of, the field-induced signal observed in measurements using the more common (a,b) plane crystal orientation may be due to the induced correlations, and not to an increase of magnetic volume fraction or ordered magnetic moments in the superconductor, as commonly believed. In the present work, we perform a comprehensive study of the field-induced signal of a LSCO crystal of a slightly larger doping level, $x = 0.12$. Our results confirm the earlier findings of both field-induced magnetism and field-induced c-axis correlations in this system. In particular, we find that much of the observed IC signal in our experiments arises from an actual increase of the magnetic moments in the system. In addition, short-range c-axis correlations develop. We present estimates for corrections of the values of field-induced signal arising due to c-axis correlations. Surprisingly, we also find that fast cooling of the crystal to base temperature induces short-range c-axis correlations similar to what is found when applying a strong magnetic field. In combination with observations by Lee *et al.* [24] on oxygen-doped La_2CuO_{4+y}, these observations

*Present address: School of Metallurgy and Materials, University of Birmingham, Edgbaston, Birmingham, United Kingdom.

suggest that fast cooling and application of a magnetic field have similar effects on the IC order.

II. EXPERIMENTAL METHOD

The $La_{1.88}Sr_{0.12}CuO_4$ sample studied in this work consisted of a single crystal grown by the traveling solvent floating zone method [25]. It exhibits a superconducting transition temperature of $T_c = 27 \pm 1.5$ K and a magnetic ordering temperature of $T_N = 30$ K [18]. In earlier work on the same crystal [18,26], the Sr content $x = 0.120 \pm 0.005$ was determined from the structural transition temperature separating the high-temperature tetragonal (HTT) from the low-temperature orthorhombic (LTO) phase. A neutron-diffraction scan of the structural (200) reflection shows that the crystal displays twinning into primarily two domains.[1] We have checked that the twin pattern is reproducible under slow-cooling conditions.

High-resolution elastic neutron-scattering experiments were carried out on three different cold-neutron triple-axis spectrometers: RITA-II [27] at the SINQ neutron source at PSI, Switzerland; FLEXX [28] at the BER2 research reactor at HZB Berlin, Germany; and PANDA at the FRM II research reactor source in Munich, Germany. Preliminary data were taken at BT-7 [29], NIST Center for Neutron Research (NCNR). We performed measurements with the sample oriented with the c axis in the scattering plane. To obtain scattering from an IC position we therefore tilted the (a,b) plane $\sim 7.8^\circ$ out of the scattering plane as illustrated in Fig. 1. Thereby we get access to wave vectors of the form $\mathbf{Q} = (H\,0.14H\,L)$ in orthorhombic notation, where $a = 5.312$ Å, $b = 5.356$ Å, and $c = 13.229$ Å. We find an IC signal at the position $\mathbf{Q}_{\rm IC} = (0.887(2), 0.124(1), L)$.

In triple-axis spectrometers, the resolution ellipsoid is elongated out of the scattering plane. This means that in common experiments, where the (a,b) plane is in the scattering plane, the intensity is enhanced by resolution integration along the c axis, along which the IC signal is broad. In the present crystal alignment with the c axis in the scattering plane we do not gain intensity by these resolution effects, and optimization of the experimental setup is required. Sample rotation scans are optimal in this situation since this limits distinct background contributions from, e.g., powder lines. All experiments were therefore carried out by sample rotation scans with the exception of a few scans close to $L = 0$ in the zero-field experiment at PANDA; see the open circles and solid black lines of Fig. 1(b) for an illustration of sample rotation scans.

The PANDA experiment was performed in zero field after a quench cooling of the crystal by 4 K/min. The experimental setup was $E_i = E_f = 5.0$ meV and we used $60'$ collimation before and after the sample. A Be filter was placed between the monochromator and the sample.

In the experiments at FLEXX and RITA-II horizontal field magnets were used. The experimental setup on RITA-II was $E_i = E_f = 4.6$ meV and the nine-blade analyzer was arranged in the monochromatic **q**-dispersive mode [30]. We used an $80'$ collimation before the sample and a Be filter with radial collimation after the sample. The sample was mounted in a

[1] We note that structural twinning is sample dependent.

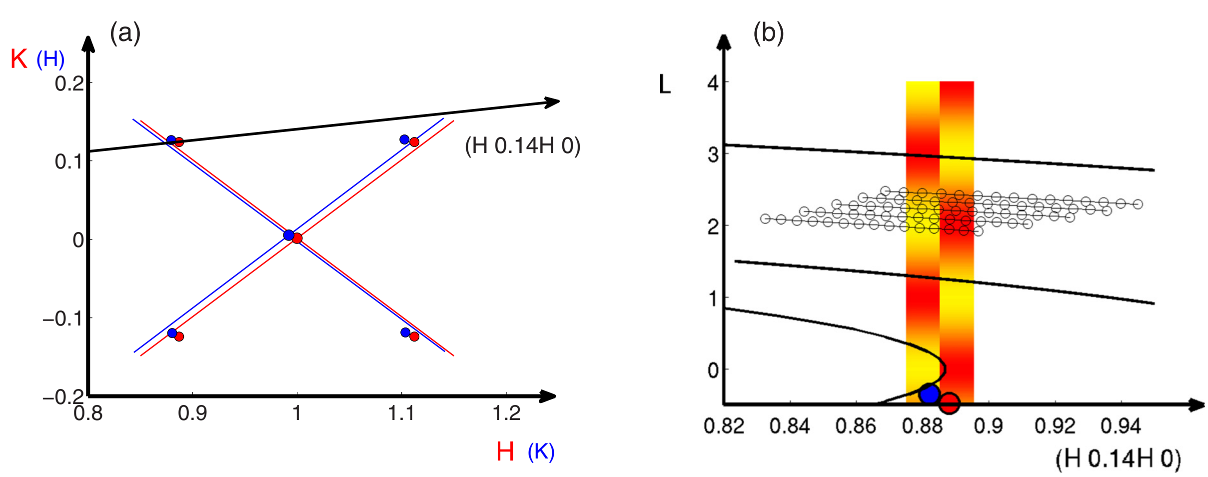

FIG. 1. (Color online) (a) Illustration of the quartet of IC peaks around (100) in orthorhombic notation. The scattering signal from the (100) structural second-order peak belonging to the dominant domain is shown by the red circle. The crystal shows twinning into two subdominant domains of which we show the strongest by the blue circles. The red and blue lines show the Cu-O-Cu axes. Note that the IC peaks are shifted off these high-symmetry axes in agreement with earlier reports [4]. The black arrow shows the axis $(H\,0.14H\,0)$, which we probe in the scattering plane. (b) Illustration of the scattering plane spanned by $(H\,0.14H\,0)$ and $(0\,0\,L)$. We show examples of a sample rotation scan through a signal rod with a proposed weak L dependence of the signal shown for the two twins of the IC signal, with maximum signal visualized by red and minimum signal shown in yellow. The width of the signals along $(H\,0.14H\,0)$ is exaggerated for clarity. Note that one twin (red circle) displays peaks at even L values and the twin shown by the blue circle exhibits peaks at odd L values. The white points visualize how the nine analyzer blades of the monochromatic **q**-dispersive mode (imaging mode) on RITA-II enable measurements at distinct values of L for one sample rotation scan. For clarity, only every second analyzer blade has been shown. The solid lines show the trajectory of the reciprocal lattice vectors in a sample rotation scan. From the scan line centered at $L = 0$, it is clear that a sample rotation scan is not applicable for small L values. With increasing L, the change in L during one sample rotation scan through the signal rod becomes smaller.

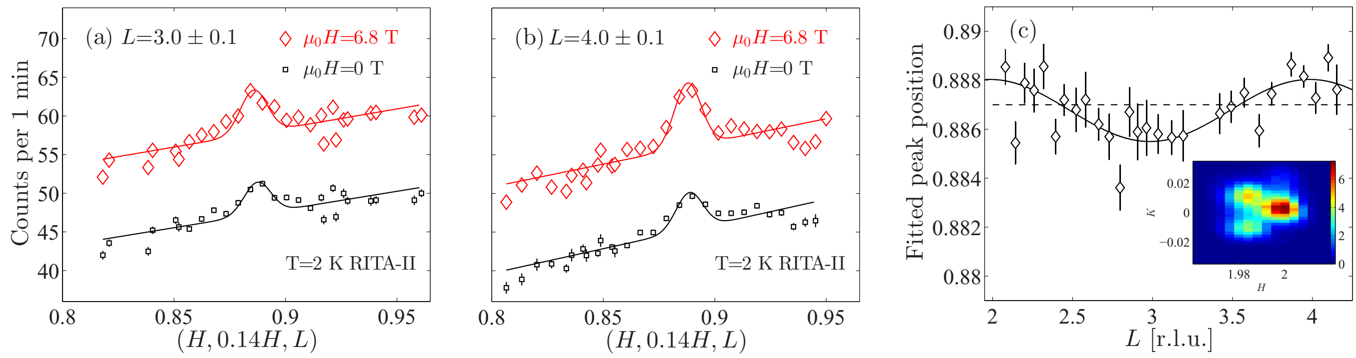

FIG. 2. (Color online) (a, b) Raw data for sample rotation scans through the IC position (H 0.14H L) for L = 3.0 and L = 4.0 in H = 6.8 T (red data points) and zero (black data points) applied field along the c direction, taken at T = 2 K. These data were taken at RITA-II, PSI. For each scan the data of five blades were combined, leading to an uncertainty in L of 0.1 r.l.u. Error bars are smaller than the marker size. The field data are shifted upwards by a constant offset for clarity. The solid curves display fits to Gaussian functions on a sloping background. (c) The fitted peak position H_{IC} for 6.8 T field data as a function of L. The dashed black line shows a fit to a straight line and the solid black line displays a fit to a sine function, which provides a better fit to the data. The color inset shows the intensity of the structural scattering signal around (200).

6.8-T horizontal field cryomagnet and data were taken in 6.8 T field applied along the c axis as well as in zero field. To improve data statistics, we performed a similar experiment at FLEXX with the sample placed in a 6-T horizontal magnet with the same orientation as in the RITA-II experiment. The FLEXX experiment was performed with energies $E_i = E_f = 5.0$ meV and we used 60′ collimation between monochromator and sample as well as between sample and analyzer. Second-order contamination from the monochromator was eliminated by a velocity selector. In both the RITA-II and FLEXX experiments the same slow sample cooling of 1 K/min was performed from T = 190 K down to T = 50 K. We studied the magnetic order by scanning through the magnetic ordering vector $\mathbf{Q}_{\text{IC}}$ at T = 2 K by rotating both the sample and the magnet, keeping the magnetic field along the c axis. In some of the scans the background contribution was estimated by performing similar scans at T = 40 K, where the magnetic order is absent.

III. RESULTS

Figures 2(a) and 2(b) show the raw data taken on RITA-II through the IC position $\mathbf{Q}_{\text{IC}}$ at different magnetic fields for L = 3 and L = 4, respectively. It is seen that for the zero-field data the peak intensity is roughly the same at L = 3 and L = 4, whereas the measurements in an applied field show a higher intensity at L = 4 than at L = 3. We fit the raw data to a single Gaussian on a sloping background keeping the width of the peak constant. The peak width is resolution limited and corresponds to a large in-plane correlation of $\xi_{\text{in-plane}} \geqslant 120$ Å , consistent with earlier measurements finding resolution-limited correlations in the (a,b) plane [18,31]. Due to the use of the monochromatic $\mathbf{q}$-dispersive mode, the RITA-II experiment amounts to almost 80 individual scans. In Figs. 2(a) and 2(b), the data of five blades are combined for an integration range of $\Delta L = 0.1$ reciprocal lattice units (r.l.u.). For the individual scans the fitted center position of the peaks varies within ≈0.002 r.l.u. around the mean value of $H_{\text{IC}} = 0.887$. Further inspection of the fitted peak center shows a clear modulation as a function of L as shown in Fig. 2(c) with $H_{\text{IC}} = 0.888$ for even L and $H_{\text{IC}} = 0.886$ for odd L. Although significant, the variation in the fitted peak center is smaller than the resolution-limited width of 0.006 r.l.u. and we cannot resolve the signal into two separate peaks. We later see that the clear modulation of the peak center provides evidence that the IC signal is twinned. In the inset of Fig. 2(c) the twinning of the structural peak at (200) is depicted, showing that three distinct structural domains are visible.

In Fig. 3 we show scans at L = 2 from the independent experiment on FLEXX. In this experiment we carefully measured the background intensity by sample rotation scans above the magnetic ordering temperature at T = 40 K and performed a pointwise background subtraction of the incommensurate magnetic signal. The figure clearly shows the effect of a 6-T magnetic field; the IC magnetic signal is roughly doubled. This is in agreement with the enhancement of the L = 0 signal in 7 T, observed in Ref. [31].

Now we turn to the main purpose of the study, which is to map out the full L dependence of the IC signal in field and in zero field. We did several scans similar to those shown

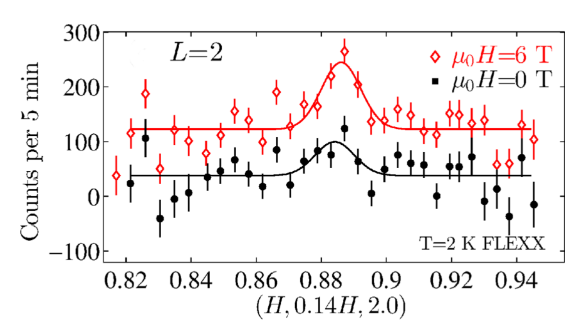

FIG. 3. (Color online) Measured peak intensity at T = 2 K for the IC position (H 0.14H 2.0) in 6 T field (red data points) and zero field (black data points). Pointwise background subtraction has been performed, using 40-K data as background. The solid curves are Gaussian fits to the data. These data were taken at FLEXX, HZB. The field data are shifted upwards by a constant offset for clarity.

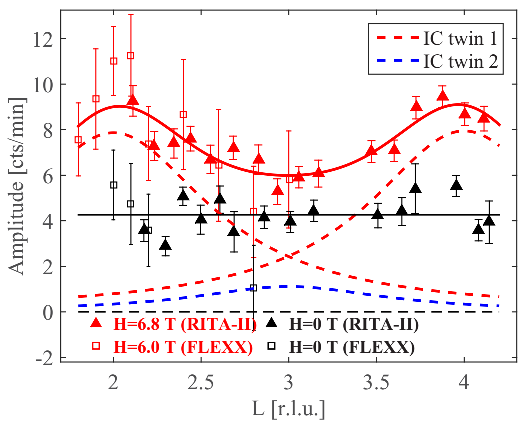

FIG. 4. (Color online) Background-subtracted elastic response at the IC position (0.887(2),0.124(1),L) versus L in zero field, a 6.0-T field (FLEXX data), and a 6.8-T field (RITA-II data). The y-axis label corresponds to the counting rate at the RITA-II experiment. To compare the two data sets, the FLEXX data have been scaled by a constant factor determined by the fraction of the signal intensities at the common data point $L = 2.2$. The red solid line corresponds to a fit to three Lorentzian functions with the same width and fixed centers at $L = 2$, 3, and 4. The three Lorentzian functions are shown separately by the red and blue dashed lines, belonging to the first and second IC twins, respectively. The color code is the same as in the cartoon drawing in Fig. 1(b).

in Figs. 2(a), 2(b), and 3 for L in the range 1.8–4.15. This span in L is significantly broader than in the previous field study in Ref. [22]. The results are summarized in Fig. 4 for both the RITA-II and FLEXX experiments. In zero field the measured IC signal is flat as a function of L; i.e., there is no observable interplanar correlations when the sample has been cooled down slowly. The effect of applying a magnetic field perpendicular to the copper oxide planes is twofold. First, weak correlations between the CuO_2 planes develop. In zero field there is no intensity modulation as a function of L, whereas a clear modulation builds up upon application of field. This is in agreement with the observations of Lake *et al.* in LSCO $x = 0.11$ [22]. Second, and more pronounced, an overall enhancement of the magnetic signal takes place for all values of L. A fit of the field data to three Lorentzian functions with same width and fixed centers at 2, 3, and 4 gives a broad modulation with half width at half maximum (HWHM) = 0.7(1) r.l.u. This corresponds to a very short correlation length of 3 Å, smaller than the distance between neighboring CuO_2 planes. Thus, the spins in neighboring planes are only very weakly correlated.

As a measure of the true enhanced intensity we integrate the signal measured in field along L and compare to the L-integrated zero-field signal. From Fig. 4 we get an L-integrated enhanced intensity of 77(8)%. For a comparison we calculate the enhancement effect at $L = 2$ from Fig. 4 and get 109(9)%. The latter corresponds to the effect which would be estimated from a measurement with the current crystal aligned in the (a,b) plane.

Finally, in Fig. 5 we show the results of the PANDA experiment, which was done at zero field, but under different experimental conditions since the crystal was quench cooled by 4 K/min. We observe a small correlation between the CuO_2 planes even when no magnetic field is applied. In this case a fit to two Lorentzian functions centered at even L, which gives a width of HWHM = 0.58(8) r.l.u., similar to the broad modulation observed in field. This leaves us with the interesting observation that quench cooling has the same qualitative effect of enhancing interplanar correlations as the application of an external magnetic field in the c direction.

IV. DISCUSSION

In the previous section we reported that c-axis correlations are absent when the system is cooled slowly from $T = 190$ K to 50 K. Further, we observed that a magnetic field as well as quench cooling can lead to the development of clear, but short-range, c-axis correlations. Now we turn to a thorough

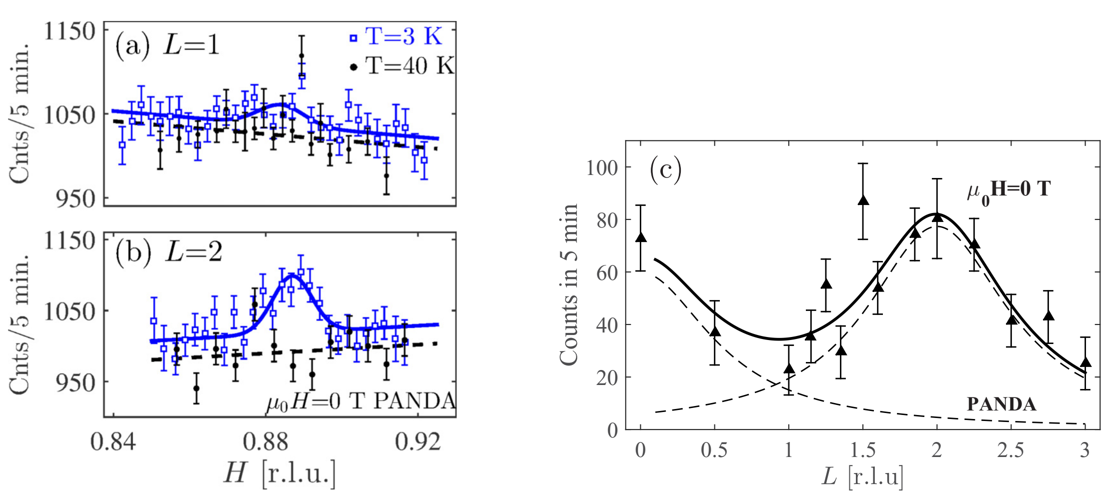

FIG. 5. (Color online) Scans through $(H\,0.14H\,L)$ at $T = 3$ K (blue open squares) and $T = 40$ K (black points) in zero field for (a) $L = 1$ and (b) $L = 2$. In both panels, the solid blue line shows a fit to a Gaussian function on a sloping background. (c) L dependence of the incommensurate magnetic signal above background in zero field measured at PANDA. The solid black line shows the fit to two Lorentzian functions with fixed centers at $L = 0$ and $L = 2$. The dashed lines show each of the Lorentzian functions separately.

discussion of the magnetic signal and how it is affected by an applied magnetic field and quench cooling the system. Finally, we discuss our experimental findings in the framework of theoretical microscopic models.

A. Peak position of the magnetic signal

We observe an IC signal at all values of L in field as well as in zero field. In field the position is at $H = 0.887(2)$ with a weak L dependence as shown in Fig. 2(c). Under the assumption that this IC signal belongs to the dominating structural twin, the mean IC position corresponds to a displacement angle of $\theta = 2.7^\circ$ away from the high-symmetry axis of the underlying CuO_2 plane. This is consistent with the findings of Kimura *et al.* [4] on a crystal of similar doping. In zero field the mean peak position is the same as in field with a slightly larger uncertainty due to the very weak signal. In zero field there is no discernible variation in peak position along L.

The signal structure along the L direction for different twin components of the IC order in LSCO has not been measured previously. Our expectations stem from the parent compound La_2CuO_4 [32,33] and superoxygenated La_2CuO_{4+y} [34]. The parent compound La_2CuO_4 displays long-range three-dimensional antiferromagnetic order with spins aligned mainly along the orthorhombic b axis [32,33]. With this spin structure the magnetic signal is peaked at *even* L for scattering at $(1\,0\,L)$ and at *odd* L for scattering at $(0\,1\,L)$. In the work by Lee *et al.* [34] the three-dimensionality of the IC signal in superoxygenated La_2CuO_{4+y} was investigated. A clear splitting of the incommensurate signal allowed measurements of IC signals centered at $(1\;0\,L)$ and $(0\,1\,L)$ simultaneously. Lee and co-workers reported the presence of incommensurate peaks, which are broad along L; for the IC signal centered at $(1\,0\,L)$ the peak is at even L while it occurs for odd L for the IC signal centered at $(0\,1\,L)$. Thus, in La_2CuO_{4+y} the arrangement of the spins in the interplanar direction bears resemblance to the spin arrangement in the parent compound with the spins being correlated across two to three CuO_2 planes [34].

In our case the orthorhombicity of the crystal is much smaller than in La_2CuO_{4+y} which makes it harder to identify a possible twinning of the IC signal. Twinning of the crystal can result in development of four different structural domains [35]. From scans through the structural peaks, three structural domains are visible as shown in the inset of Fig. 2(c). The subdominant second-order peak close to $(1\,0\,0)$ is displaced from the dominant peak by 0.8% in both directions. This corresponds to a rotation of 0.22° between the two twins. In Ref. [4] the twin splitting was reported to be $\sim 0.3^\circ$.

By a rotation of 0.22° and a rescaling of the vector length, the structural peak of the dominant twin is brought to the same position as the structural peak of the subdominant twin. Performing the same transformation on the IC peak at (0.888,0.124,0) we might expect an IC twin at the position (0.879,0.126,0). This predicts a larger deviation in peak center than expected from the lower value of the fitted peak center shown in Fig. 2(c) for $L = 3$, which is $H = 0.886$. Note, however, that the expected difference in peak position of the two IC twin signals is of the order of the resolution limitation of 0.006 r.l.u. Due to this resolution limitation along the $(H\,0.14H\,0)$ axis and due to the broadness of the signals along the $(0\,0\,L)$ axis, both IC twin signals will contribute for all values of L. Since we measure the IC signal centered at $(1\,0\,L)$ defined with respect to the dominant structural domain we expect interplanar correlations from the dominant twin to be peaked at even L. The subdominant twin signal is centered at $(0\,1\,L)$ and will therefore be peaked at odd L. Thus, the IC twin centered at (0.888,0.124,0) will dominate at even L and the other twin appears with weak intensity at odd L. The individual contributions to the field intensity are visualized by the dashed lines in Fig. 4. Since the twin which shows correlations peaked at even L is more pronounced than the twin with correlations peaked at odd L, the total signal displays peaks at even $L = 2$ and 4, whereas the peak at $L = 3$ is masked by the tails of the other two. Due to the broadness of the signals, the peak position is an average over both twins at all values of L. This is why we observe only a very small shift in the fitted peak center as a function of L shown in Fig. 2(c). Our observations are consistent with this picture.

B. Field-induced *c*-axis correlations

From the two independent field experiments done at RITA-II and FLEXX we find that the IC signal at $(0.887{,}0.124{,}L)$ is enhanced by a magnetic field at all values of L, but in particular for even L. The results of both experiments agree on the magnitude of the magnetic field enhancement at even L which is close to a factor of 2 in both cases.

Although the FLEXX experiment provided fewer data points, it is clear from Fig. 4 that both experiments agree on the development of weak interplanar correlations in a field as reflected in the L dependence of the amplitude of the IC intensities. The peaks which are centered at even values of L are very broad and the correlation length is smaller than the interplanar distance of 6.5 Å. This deviates from the correlation length of more than 10 Å as found in Ref. [22] for LSCO $x = 0.11$. We note that the correlation length determined in Ref. [22] is likely uncertain due to the sparse data. However, we cannot rule out a real difference in the field-induced interplanar correlation length between these two crystals of different doping levels. Since our crystal displays enhanced magnetic order in zero field compared to smaller doping values [18], it might be harder to induce the interplanar correlations by a field.

The primary effect of an applied magnetic field is to enhance the magnetic signal by enlarging either the magnetic volume fraction or the ordered magnetic moments. In principle, rotation of the spins could give rise to an enhancement of the magnetic signal at $L = 0$, but this was ruled out by the study by Lake *et al.* [22]. Our neutron-scattering experiment does not allow for a distinction between an enlarged magnetic volume fraction or increased ordered magnetic moments. Muon spin-rotation studies on the same crystal show that magnetic order is present throughout the entire volume of the sample with a resolution of 20 Å given by the effective range over which a muon is sensitive to the presence of static electronic moments [18,36], and we conclude that the main effect arises from enlargening of the ordered magnetic moments.

In addition, development of weak interplanar correlations occurs as a response to the applied magnetic field. As a consequence, the field effect reported in the literature on magnetism in the cuprates that has been measured in the usual configuration $L = 0$ must be requantified, since it is either over- or underestimated, depending on whether the dominant IC peak belongs to a "(100)" or "(010)" IC quartet. For our crystal, measuring at the IC peak at (0.887,0.124,0) with $L = 0$ would cause an overestimation of the field effect. At even L the amplitude enhancement is roughly 109%, whereas the real increase of magnetic order measured from the L-averaged intensity is only 77%. Thus, the field effect is overestimated by 40%.

C. Cooling-induced *c*-axis correlations

Another new finding in this work is the fact that interplanar correlations are also found in zero field under different experimental conditions where the crystal is quench cooled from room temperature down to base temperature below 4 K. In contrast to the experiments on RITA-II and FLEXX, where the temperature regime for ordering of possible excess oxygen was traversed slowly, this was passed extremely fast in the PANDA zero-field experiment. This is likely to have resulted in finite interplanar correlations as evident from Fig. 5, qualitatively similar to the result of an applied magnetic field.

To understand this behavior, we first compare our sample to superoxygenated crystals where the excess oxygen ions order in a three-dimensional structure upon slow cooling. Lee *et al.* [24] showed that fast cooling leads to an oxygen-disordered state displaying enhanced spin-density-wave (SDW) order compared to the oxygen-ordered state. In fact, in this work it was observed that disordering the excess oxygen has the same enhancement effect of the SDW signal as the application of a 7.5-T field. However, it remains unknown how disordered oxygen ions or applied magnetic field affect the magnetic correlations between the CuO_2 planes.

In this paper we show that the cooling history can be important for the interplanar correlations and thereby also affect the strength of the IC signal when measured in the $L = 0$ configuration. We put forward a possible explanation for our observations. The sample might have a small amount of excess oxygen since this is not easily avoided during crystal growth. Fast cooling through the temperature regime where ordering of possible excess oxygen takes place, which occurs down to $\sim$180 K, might cause random positions of the excess oxygen ions. Such impurities could act as pinning centers enhancing the magnetic correlations between the planes.

D. Theoretical scenario

Theoretically, the slowing down and subsequent pinning of static magnetic order by disorder sites and twin boundaries [37–46] and vortices [47–53] has been previously discussed extensively in the literature. From the microscopic studies, it is clear that the modulations of charge density and/or electron hopping amplitudes induced by impurities and twin boundaries can lead to local magnetic instabilities which nucleate magnetic order in the vicinity of the perturbing sites. The vortices, on the other hand, typically induce local magnetic order due to the suppressed superconducting gap and an associated enhanced local density of states near the Fermi level in the cores. It has been shown that even in strongly disordered situations vortices enhance the in-plane magnetic moments [53,54]. To the best of our knowledge, the out-of-plane induced magnetic order by disorder or by vortices has not been described by microscopic models, and constitutes an interesting future study. For the pure superconducting system, flux lines along the c axis should lead to substantially enhanced spin correlations along L [22]. The weak coupling between the CuO_2 planes will lead to short-ranged vortex-induced magnetic order, but the extremely short c-axis correlations found here point to additional effects. Certainly, the full magnetic volume fraction already in zero field indicates that there is hardly any "room" for vortices to induce coherent spin correlations along the c axis. Instead, the vortices lead to local enhancements of the magnetic moments and presumably adapt to the many preexisting pinning centers and strongly meander along c, leading to only very weak c-axis field-induced correlations in qualitative agreement with our observations. Within this scenario, samples with less static magnetic order in zero field should lead to longer-ranged and more pronounced c-axis correlations in the presence of a magnetic field.

V. CONCLUSIONS

We have studied the field dependence of the interplanar magnetic correlations in $La_{1.88}Sr_{0.12}CuO_4$. The primary effect of an applied magnetic field is an enhancement of the magnetic moments. Further, there is an effect of increased interplanar correlations in the presence of an applied field. The interplanar correlation length is very small and implies correlations only between neighboring planes. This indicates that the magnetic order is already strongly pinned by impurities in the sample and that vortices tend to bend rather than go perpendicular to the CuO_2 planes on the way through the sample. We observe that a fast-cooling procedure results in the same feature as application of a magnetic field, namely development of weak interplanar correlations. One possible scenario caused by excess oxygen could lead to pinning of the magnetic order between the CuO_2 planes thereby explaining why a quench-cooled system behaves similarly as a system subjected to an external field.

ACKNOWLEDGMENTS

We are grateful for the access to neutron beam time at the neutron facilities at NCNR, BER-2 at Helmholtz-Zentrum Berlin, FRM II at MLZ Garching, and SINQ at the Paul Scherrer Institute. This project was supported by the Danish Council for Independent Research through DANSCATT and by Grant No. 0602-01982B. B.M.A. acknowledges support from the Lundbeckfond (Fellowship Grant No. A9318).

[1] M. Vojta, Adv. Phys. **58**, 699 (2009); D. C. Johnston, *ibid.* **59**, 803 (2010).
[2] R. J. Birgeneau, D. R. Gabbe, H. P. Jenssen, M. A. Kastner, P. J. Picone, T. R. Thurston, G. Shirane, Y. Endoh, M. Sato, K. Yamada, Y. Hidaka, M. Oda, Y. Enomoto, M. Suzuki, and T. Murakami, Phys. Rev. B **38**, 6614 (1988).
[3] R. J. Birgeneau, Y. Endoh, K. Kakurai, Y. Hidaka, T. Murakami, M. A. Kastner, T. R. Thurston, G. Shirane, and K. Yamada, Phys. Rev. B **39**, 2868 (1989).
[4] H. Kimura, H. Matsushita, K. Hirota, Y. Endoh, K. Yamada, G. Shirane, Y. S. Lee, M. A. Kastner, and R. J. Birgeneau, Phys. Rev. B **61**, 14366 (2000).
[5] J. M. Tranquada, in *Handbook of High-Temperature Superconductivity Theory and Experiment*, edited by J. R. Schrieffer (Springer, New York, 2007).
[6] R. J. Birgeneau, C. Stock, J. M. Tranquada, and K. Yamada, J. Phys. Soc. Jpn. **75**, 111003 (2006).
[7] K. Yamada, C. H. Lee, K. Kurahashi, J. Wada, S. Wakimoto, S. Ueki, H. Kimura, Y. Endoh, S. Hosoya, G. Shirane, R. J. Birgeneau, M. Greven, M. A. Kastner, and Y. J. Kim, Phys. Rev. B **57**, 6165 (1998).
[8] S. Katano, M. Sato, K. Yamada, T. Suzuki, and T. Fukase, Phys. Rev. B **62**, R14677 (2000).
[9] Q. Li, M. Hücker, G. D. Gu, A. M. Tsvelik, and J. M. Tranquada, Phys. Rev. Lett. **99**, 067001 (2007).
[10] J. M. Tranquada, G. D. Gu, M. Hücker, Q. Jie, H.-J. Kang, R. Klingeler, Q. Li, N. Tristan, J. S. Wen, G. Y. Xu, Z. J. Xu, J. Zhou, and M. V. Zimmermann, Phys. Rev. B **78**, 174529 (2008).
[11] M. Hücker, M. V. Zimmermann, G. D. Gu, Z. J. Xu, J. S. Wen, G. Xu, H. J. Kang, A. Zheludev, and J. M. Tranquada, Phys. Rev. B **83**, 104506 (2011).
[12] H.-H. Wu, M. Buchholz, C. Trabant, C. F. Chang, A. C. Komarek, F. Heigl, M. v. Zimmermann, M. Cwik, F. Nakamura, M. Braden, and C. Schüßler-Langeheine, Nat. Comm. **3**, 1023 (2012).
[13] N. B. Christensen, J. Chang, J. Larsen, M. Fujita, M. Oda, M. Ido, N. Momono, E. M. Forgan, A. T. Holmes, J. Mesot, M. Huecker, and M. v. Zimmermann, arXiv:1404.3192.
[14] V. Thampy, M. P. M. Dean, N. B. Christensen, L. Steinke, Z. Islam, M. Oda, M. Ido, N. Momono, S. B. Wilkins, and J. P. Hill, Phys. Rev. B **90**, 100510(R) (2014).
[15] T. P. Croft, C. Lester, M. S. Senn, A. Bombardi, and S. M. Hayden, Phys. Rev. B **89**, 224513 (2014).
[16] T. Suzuki, T. Goto, K. Chiba, T. Shinoda, T. Fukase, H. Kimura, K. Yamada, M. Ohashi, and Y. Yamaguchi, Phys. Rev. B **57**, R3229 (1998).
[17] B. Lake, H. M. Rønnow, N. B. Christensen, G. Aeppli, K. Lefmann, D. F. McMorrow, P. Vorderwisch, P. Smeibidl, N. Mangkorntong, T. Sasagawa, M. Nohara, H. Takagi, and T. E. Mason, Nature (London) **415**, 299 (2002).
[18] J. Chang, Ch. Niedermayer, R. Gilardi, N. B. Christensen, H. M. Rønnow, D. F. McMorrow, M. Ay, J. Stahn, O. Sobolev, A. Hiess, S. Pailhés, C. Baines, N. Momono, M. Oda, M. Ido, and J. Mesot, Phys. Rev. B **78**, 104525 (2008).
[19] M. Kofu, S.-H. Lee, M. Fujita, H.-J. Kang, H. Eisaki, and K. Yamada, Phys. Rev. Lett. **102**, 047001 (2009).
[20] J. Chang, N. B. Christensen, Ch. Niedermayer, K. Lefmann, H. M. Rønnow, D. F. McMorrow, A. Schneidewind, P. Link, A. Hiess, M. Boehm, R. Mottl, S. Pailhés, N. Momono, M. Oda, M. Ido, and J. Mesot, Phys. Rev. Lett. **102**, 177006 (2009).
[21] B. Khaykovich, S. Wakimoto, R. J. Birgeneau, M. A. Kastner, Y. S. Lee, P. Smeibidl, P. Vorderwisch, and K. Yamada, Phys. Rev. B **71**, 220508(R) (2005).
[22] B. Lake, K. Lefmann, N. B. Christensen, G. Aeppli, D. F. McMorrow, H. M. Rønnow, P. Vorderwisch, P. Smeibidl, N. Mangkorntong, T. Sasagawa, M. Nohara, and H. Takagi, Nat. Mater. **4**, 658 (2005).
[23] The doping of the crystal in Ref. [22] was later shown to be closer to $x = 0.11$ rather than $x = 0.10$ from a measurement of the transition temperature from HTT to LTO [26].
[24] Y. S. Lee, F. C. Chou, A. Tewary, M. A. Kastner, S. H. Lee, and R. J. Birgeneau, Phys. Rev. B **69**, 020502(R) (2004).
[25] T. Nakano, N. Momono, M. Oda, and M. Ido, J. Phys. Soc. Jpn. **67**, 2622 (1998).
[26] R. Gilardi, Ph.D. dissertation no. 15780, ETH Zürich, 2004.
[27] C. R. H. Bahl, P. Andersen, S. N. Klausen, and K. Lefmann, Nucl. Instrum. Methods Phys. Res., Sect. A **226**, 667 (2004).
[28] M. D. Le, D. L. Quintero-Castro, R. Toft-Petersen, F. Groitl, M. Skoulatos, K. C. Rule, and K. Habicht, Nucl. Instrum. Methods Phys. Res., Sect. A **729**, 220 (2013).
[29] J. W. Lynn, Y. Chen, S. Chang, Y. Zhao, S. Chi, W. Ratcliff II, B. G. Ueland, and R. W. Erwin, J. Res. Natl. Inst. Stand. Technol. **117**, 61 (2012).
[30] C. R. H. Bahl, K. Lefmann, A. B. Abrahamsen, H. M. Rønnow, F. Saxild, T. B. S. Jensen, L. Udby, N. H. Andersen, N. B. Christensen, H. S. Jacobsen, T. Larsen, P. S. Häfliger, S. Streule, and Ch. Niedermayer, Nucl. Instrum. Methods Phys. Res., Sect. B **246**, 452 (2006); K. Lefmann, Ch. Niedermayer, A. B. Abrahamsen, C. R. H. Bahl, N. B. Christensen, H. S. Jacobsen, T. L. Larsen, P. Häfliger, U. Filges, and H. M. Rønnow, Phys. B (Amsterdam, Neth.) **385-386**, 1083 (2006).
[31] A. T. Rømer, J. Chang, N. B. Christensen, B. M. Andersen, K. Lefmann, L. Mähler, J. Gavilano, R. Gilardi, Ch. Niedermayer, H. M. Rønnow, A. Schneidewind, P. Link, M. Oda, M. Ido, N. Momono, and J. Mesot, Phys. Rev. B **87**, 144513 (2013).
[32] D. Vaknin, S. K. Sinha, D. E. Moncton, D. C. Johnston, J. M. Newsam, C. R. Safinya, and H. E. King, Jr., Phys. Rev. Lett. **58**, 2802 (1987).
[33] Y. Endoh, K. Yamada, R. J. Birgeneau, D. R. Gabbe, H. P. Jenssen, M. A. Kastner, C. J. Peters, P. J. Picone, T. R. Thurston, J. M. Tranquada, G. Shirane, Y. Hidaka, M. Oda, Y. Enomoto, M. Suzuki, and T. Murakami, Phys. Rev. B **37**, 7443 (1988).
[34] Y. S. Lee, R. J. Birgeneau, M. A. Kastner, Y. Endoh, S. Wakimoto, K. Yamada, R. W. Erwin, S.-H. Lee, and G. Shirane, Phys. Rev. B **60**, 3643 (1999).
[35] M. Braden, G. Heger, P. Schweiss, Z. Fisk, K. Gamayunov, I. Tanaka, and H. Kojima, Phys. C (Amsterdam, Neth.) **191**, 455 (1992).
[36] J. Larsen, Ph.D. dissertation, Technical University of Denmark, 2013.
[37] H. Tsuchiura, Y. Tanaka, M. Ogata, and S. Kashiwaya, Phys. Rev. B **64**, 140501(R) (2001).
[38] Z. Wang and P. A. Lee, Phys. Rev. Lett. **89**, 217002 (2002).
[39] J.-X. Zhu, I. Martin, and A. R. Bishop, Phys. Rev. Lett. **89**, 067003 (2002).
[40] Y. Chen and C. S. Ting, Phys. Rev. Lett. **92**, 077203 (2004).
[41] H. Kontani and M. Ohno, Phys. Rev. B **74**, 014406 (2006).
[42] J. W. Harter, B. M. Andersen, J. Bobroff, M. Gabay, and P. J. Hirschfeld, Phys. Rev. B **75**, 054520 (2007).

[43] B. M. Andersen, P. J. Hirschfeld, A. P. Kampf, and M. Schmid, Phys. Rev. Lett. **99**, 147002 (2007).
[44] B. M. Andersen, S. Graser, and P. J. Hirschfeld, Phys. Rev. Lett. **105**, 147002 (2010).
[45] R. B. Christensen, P. J. Hirschfeld, and B. M. Andersen, Phys. Rev. B **84**, 184511 (2011).
[46] U. Tricoli and B. M. Andersen, J. Supercond. Novel Magn. **25**, 1329 (2012).
[47] D. P. Arovas, A. J. Berlinsky, C. Kallin, and S.-C. Zhang, Phys. Rev. Lett. **79**, 2871 (1997).
[48] B. M. Andersen, H. Bruus, and P. Hedegård, Phys. Rev. B **61**, 6298 (2000).
[49] E. Demler, S. Sachdev, and Y. Zhang, Phys. Rev. Lett. **87**, 067202 (2001).
[50] Y. Chen and C. S. Ting, Phys. Rev. B **65**, 180513(R) (2002).
[51] M. Takigawa, M. Ichioka, and K. Machida, Phys. Rev. Lett. **90**, 047001 (2003).
[52] B. M. Andersen, O. F. Syljuåsen, and P. Hedegard, Phys. Rev. B **80**, 052509 (2009).
[53] B. M. Andersen, S. Graser, M. Schmid, A. P. Kampf, and P. J. Hirschfeld, J. Phys. Chem. Solids **72**, 358 (2011).
[54] M. Schmid, B. M. Andersen, A. P. Kampf, and P. J. Hirschfeld, New J. Phys. **12**, 053043 (2010).